Resolution Degradation in X-ray Detectors based on Superconducting Tunnel Junctions

Roland den Hartog, P. Verhoeve, A. Peacock, A. Poelaert, N. Rando
Astrophysics Division, Space Science Department of the European Space Agency at ESTEC, the Netherlands

Abstract—**Despite considerable progress over the past years, the detection of medium-energy X-ray photons (E > 1 keV) with STJs near the energy-resolution limit, set by the Fano and tunnel noise, remains an elusive goal. There is presently little doubt that the spatially inhomogeneous response of the STJ is responsible for the degradation of the energy resolution. We review several proposed mechanisms against experimental data for Nb- and Ta-based STJs, of various sizes and in single or array-format. We argue against a single mechanism behind the resolution degradation. The experimental results presented here support a model in which quasi-particles are lost at the edges of the STJ, but also indicate that losses into the leads seriously degrade the energy resolution. Finally, an example is given of how fabrication details may play a role as well.**

I. Introduction

Arrays of detectors based on Superconducting Tunnel Junctions (STJs) provide the possibility to perform non-dispersive, high-resolution imaging spectroscopy in a very broad range of wavelengths. Practical instruments for optical, UV and soft X-ray (< 1 keV) wavelengths are now feasible through the successful development of small-format STJ arrays, with up to 6×6 pixels (see Fig. 1) [1]. At soft X-ray wavelengths energy resolutions to within a factor ~2 above the statistical limit have been found for Ta-based STJs (i.e. ΔE = 3.4 eV (FWHM) for 525 eV photons) [2, 3], but at higher X-ray energies the situation is less satisfactory.

The energy resolution of an STJ is usually approximated as the Gaussian sum of the following factors:

$$\Delta E = 2.355\,[\sigma^2_{Fano} + \sigma^2_{tun} + \sigma^2_{el} + \sigma^2_{spat}]^{1/2}. \quad (1)$$

Here σ_{Fano} is the Fano-limited resolution, the statistical fluctuation in the initial number of quasi-particles (QPs) created immediately after the photo-absorption [4, 5], and σ_{tun} is the fluctuation in the number of electrons that actually tunnel across the barrier [6, 7]. Both are proportional to $E^{1/2}$ and the Gaussian sum of these two factors forms the statistical limit on the energy resolution of STJs. σ_{el} is the noise contributed by the electronics and the surroundings, which is assumed to be independent of E. σ_{spat} represents the spatial non-uniformity in the charge response Q of the STJ, and is generally considered to be directly propertional to E.

The central question in the research presented here is the physical origin of the spatial variation of Q. The results presented here demonstrate that different mechanisms can lead to very similar spatial response functions. Detailed knowledge of these physical mechanisms is essential in the selection of an effective strategy to improve the resolution.

Manuscript received September 15, 1998

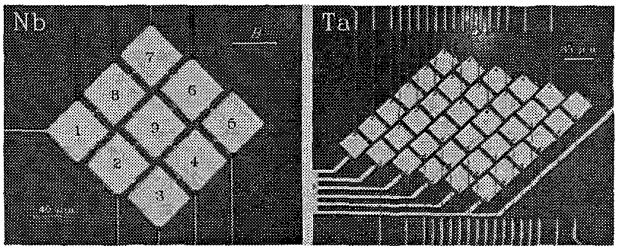

Fig. 1. Top view microscope images of a 3×3 test array of Nb-based STJs (left) and a 6×6 Ta-based array (right). The (square) Nb-based STJs have a size of 40 μm, the (also square) Ta-based STJs have a size of 25 μm. Note that the top electrode of the central pixel (no. 9) of the Nb array is not connected. The base electrodes of adjacent STJs are connected via bridges. While in the Nb array the number of bridges is 2 or 3, depending on position, it is 2 for all pixels in the Ta array. The widths of the electrical connections to the top films are 1.5 μm in the Ta array, and in the Nb array resp. 1 μm for STJs 1, 6, 7 and 8 (top row), and 2 μm for STJs 2, 3, 4 and 5 (bottom row). In both arrays, the material of the bridges and leads is Nb.

II. Experimental Results

A. Some experimental details

The results presented here are based on several types of measurements on a variety of different STJs, so space does not permit us to discuss all the experiments in detail. A more detailed description of the experiments is presented elsewhere [1, 2, 3, 8, 9]. Nevertheless, the lay-out of the STJs discussed here is quite uniform. The Nb-based STJs consist of a multi-layer of a 100 nm epitaxial Nb base film, sputtered on a super-polished sapphire substrate, a ~10 nm thick epi-Al / AlOx / poly-Al barrier layer and a 200 nm poly-crystalline Nb top film. The Ta-based STJs have instead a 100 nm poly-crystalline Ta top film. Each detector chip carries 8 to 10 single square STJs, with sizes L in the range 10 – 200 μm, or a single array as shown in Fig. 1. The operating temperature is 0.3 – 0.4 K.

B. The magnitude of the spatial response inhomogeneity

Although we know from the analysis of spectral-line profiles that the Gaussian approximation breaks down for large contributions from σ_{spat} [10, 11], (1) provides an acceptable approximation. This is shown in Fig. 2, where ΔE is plotted as a function of E for STJs from the arrays shown in Fig. 1. The spatial non-uniformity of Q dominates the resolution above a few 100 eV, even though the magnitude of the variations is of the order of 1% of the charge output.

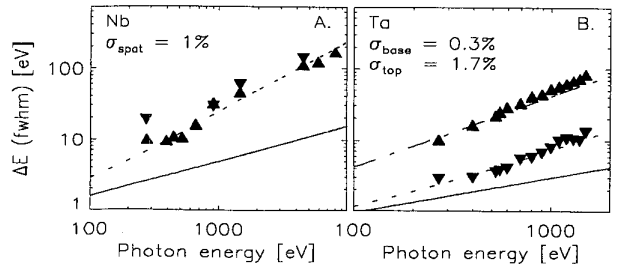

Fig. 2. The energy resolution as a function of photon energy, for both top film (▲) and base film (▼). Data points are presented for one pixel of the Nb 3x3 array (left) and as an average of 3 pixels for the Ta 6×6 array (right). The energy resolutions plotted here have been corrected for electronic noise. Solid lines indicate the statistical limit from Fano and tunnel noise, dashed lines correspond to a best fit model including the contribution from the spatial non-uniformity of the charge response. The size of these non-uniformities, σ_{spat}, defined as per cent RMS variations from the mean, is also indicated.

A 6 keV energy resolution to within a factor 2 from the statistical limit requires a spatial uniformity in the charge response better than ~0.1%. We are approaching this goal for the Ta base film, but for the top films there is still an order of magnitude to be gained.

C. *Energy resolution as a function of device size*

From Fig. 3 it is apparent that the spatial inhomogeneity has a large geometrical component. The difference in the behaviour of ΔE between the epitaxial base film and the poly crystalline top film, in both Nb and Ta, is quite remarkable, particularly because Q increases with increasing device size for both electrodes. This is to be expected when the main QP losses take place at the edges.

The SRON group [10, 11] has developed a phenomenological diffusion model that represents the QP trapping at the edges by a reflectivity R slightly less than 1. Fig. 4 shows

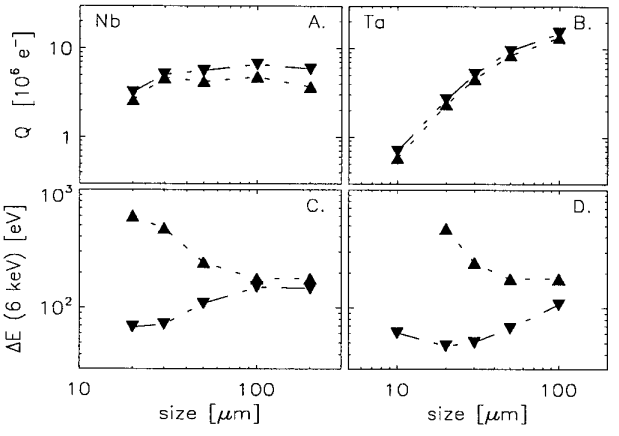

Fig. 3. Charge output Q (top row) and energy resolution ΔE (bottom row) for both top film (▲) and base film (▼) as a function of STJ size, measured for series of single STJs based on Nb (left) and Ta (right). Data points are averages of several series of STJs.

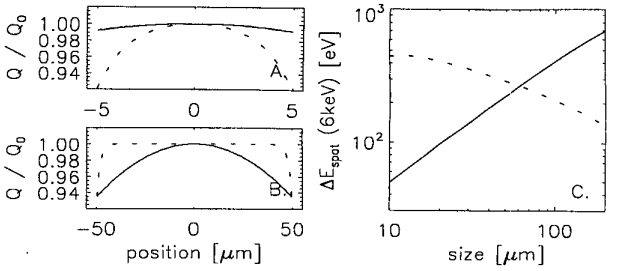

Fig. 4. Illustrations of the response profiles predicted by the SRON model, for the base (solid line) and top film (dashed line) of a 10 μm (a) and a 100 μm (b) STJ. Q_0 is the charge response in the center of the STJ. On the right hand ΔE as a function of device size, based on this model. To be compared with Fig. 3c.

that this model can explain, at least qualitatively, the behaviour of ΔE for both films seen in Figs. 3c and d. The model parameters are edge reflectivity R, the QP mean free path ℓ, which is estimated from the low-temperature resistivity of the film, and the ratio Λ/L between the mean distance over which a QP diffuses during its lifetime τ_{life} and the size of the STJ. For Fig. 4 we took values typical for our Nb STJs in Fig. 3. In order to have ΔE_{top} decrease with size, Λ_{top} had to be taken a factor 30 smaller than its estimate $[2D\tau_{life}]^{1/2} \approx 30$ μm. While ℓ is equal to the diameter of the columnal grains in poly-Nb (~30 nm, determined with TEM), the actual diffusion of QPs appears much slower. Such an effect has been reported before, both for poly-crystalline Nb and Ta [11, 12, 13]. Following [13], we speculate this is due to Andreev reflections of QPs at the grain boundaries, which make the QP trajectory less effective than a classical random walk with mfp ℓ.

The SRON model was originally motivated by a scenario in which NbO forms at the edges of the Nb-based STJs as the result of natural oxidation. Because NbO has a lower bandgap energy than Nb, the oxidized sites act as QP traps, thus providing the loss mechanism at the edges. However, the model applies equally well to Ta-based STJs, although none of the Ta-oxides are superconducting. In particular, the change from Nb to Ta as the main electrode material did not bring a large improvement in the STJ energy resolution [3, 10, 14, 15, and Fig. 3a, b]. It did, however, make a differences for the charge response, presumably because trapping losses from NbOx at the surface of the top electrode were eliminated. A similar improvement of Q could be obtained by covering the top electrode of a Nb STJ with a 5 nm layer of NbN, which has a higher bandgap than Nb and thus repels QPs [16]. So it seems that the QP trapping does have an effect, but not so much on the energy resolution.

D. *Influence of leads*

Fig. 5 presents a set of measurements on the individual STJs in the 3×3 Nb array. The charge output depends mainly on the number of base-film bridges; on average 7% of QPs

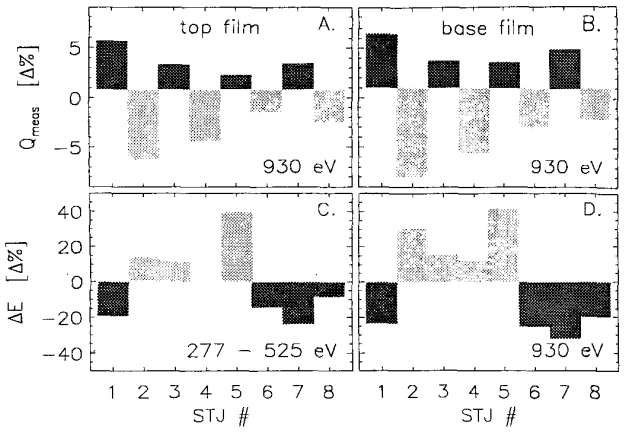

Fig. 5. Per cent deviations from the mean of charge output and energy resolution of the 8 connected pixels in the Nb 3×3 array shown in Fig. 1a. The top row panels demonstrate that the charge output of both the top and the base film varies with the number of bridges connecting to the base electrode (dark shading: 2; light shading: 3). Per bridge, on average 7% of the quasi-particles are lost to the adjacent STJ. The bottom row shows that the energy resolution is practically independent of the number of base-film bridges, but strongly depends on the width of the top lead. Here dark shading indicates a width of 1μm, and light shading a width of 2 μm. The top-film resolution was measured at a range of energies for which all photons were absorbed in the top film.

diffuses across each bridge. This was confirmed by charge-output measurements with electronics that simultaneously read out adjacent pixels. However, the energy resolution hardly depends on number of base film bridges at all, but correlates strongly with the width of the top lead. Reduction of the width by 50% improves ΔE on average by 40%.

This result is not a complete surprise. An LTSEM measurement on one of our earlier Nb-based devices also shows a major impact of the contact lead on the homogeneity of the signal response of the STJ [12]. This effect was stronger than the influence from QP losses at the edges.

A potential remedy for the resolution reduction by the leads is to prevent QPs entering the leads by the application of materials with a higher bandgap energy Δ than the electrode. We found it possible to improve ΔE_{base} of the Nb-based 20 μm STJ described in [17] by 30% and ΔE_{top} by 50%, by inserting NbN plugs in the leads.

For Ta-based STJs the lead problem is not so easily solved. The 6×6 Ta array has Nb bridges, but still 7% of the QPs escapes across the 4 μm bridge, the same fraction as in the 3×3 Nb array which has unmodified bridges. *Somehow, QPs can escape into higher bandgap material.* This finding ties in with a comparison of two identical Ta-based STJs, one with Ta and one with Nb leads, which did not show an improvement of ΔE for the STJ with Nb leads, just like the number of base-film bridges did not influence ΔE in the 3×3 Nb array. It is a well-known fact that QPs can gain an energy of eV_{bias} (~0.25Δ in our experiments) from the tunnel and back-tunnel processes [18]. In our Ta-based STJs, the number of tunnel processes per QP, $\langle n \rangle$, lies in the range of 4 to 7 for 25 μm STJs [3], so the bandgap difference between Nb and Ta (a factor of 2.3) can be easily bridged. A serious problem with this hypothesis is, however, that the scattering lifetime of QPs with energies above Δ is much shorter (< 1 ns) than the tunnel time (~1 μs) [19, see also 16]. QPs with an energy of 2Δ can travel ~7 μm in our epitaxial Ta films before being scattered into a lower energy state. Hence, a possible alternative explanation is that QPs created directly after the photo-absorption process, when the energy is still ≥ 2Δ, are able to escape from the electrode, provided the absorption takes place close enough to the base lead.

Work is currently in progress to incorporate diffusion into the leads and edge trapping of QPs in a numerical model based on the Rothwarf-Taylor equations. The situation may not be too different from QP trapping at the edges, except that instead of many small trapping sites we now have one big loss channel. Of course, the actual solution at the fabrication level requires an entirely different approach.

E. Spatial variations of the bandgap

Fig. 6a demonstrates that in our series of single Nb-based STJs there is a clear correlation between the bandgap Δ, as obtained from the I-V characteristics, and the size of the STJ. The observed 4% decrease in Δ over the range of sizes, implies that Δ increases towards the edge of a STJ. The Ta-based STJs do not show this variation of Δ with size, as is clear from Fig. 6b. The reason for this can be seen in the TEM cross-section photos of edge regions in Fig. 7. During the etch process, Al is etched away faster than Nb. As a result, the edge of the Nb-based STJs has a serration, typically 200 nm deep, centered at the Al layer. The 200 nm wide rim is not in direct contact with the Al, and therefore the local Δ_{Nb} above and below the rim is less influenced by the proximity effect. Clearly, the Ta-based STJs do not suffer from this problem. Fig. 8a illustrates several phenomenological models of the variation of Δ with distance to the edge d, where the variation is assumed to be independent of the size of the STJ. The variation in the charge response follows from $Q = E / (1.74\ \Delta)$. The contribution to the resolution that

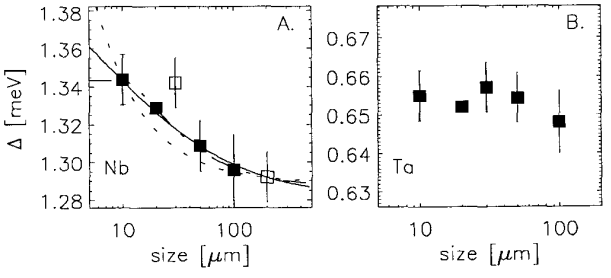

Fig. 6. The measured bandgap Δ as a function of device size for series of single Nb- and Ta-based STJs. Open symbols in the right panel indicate data points based on one measurement only. The various curves correspond to models detailed in Fig. 8.

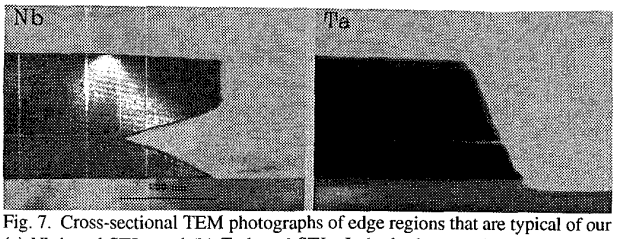

Fig. 7. Cross-sectional TEM photographs of edge regions that are typical of our (a) Nb-based STJs, and (b) Ta-based STJs. In both photographs the central 10 nm thick sandwich of Al/AlOx/Al is visible as a bright line. The serration in the Nb edge at the position of the Al layer is ~200 nm deep.

results from this response inhomogeneity is given as a function of device size in Fig. 8b. Each of these models were fit to the data in Fig. 6a. Given the error bars, the data does not strongly distinguish between these models. Considering the correlation length in Nb, $\xi_0 \approx 40$ nm, the physically most plausible model is the one where Δ steps at 200 nm from the edge. However, the ΔE predicted by this model is much higher than we have measured, in particular for the smaller devices. A comparison between Figs. 3c and 8b suggests that all models are more suitable for the top film than for the base film. This would imply that the bandgap gradient is stronger in the top film than in the base film, which can be qualitatively understood in terms of the Golubov model of the proximity effect [20, 21]. In the presence of a resistive barrier, such as formed by the network of grain boundaries in the poly-crystalline top film, much larger bandgap gradients are possible than in a highly conductive medium, such as the epitaxial base film. Curiously, the best fitting model, $\Delta \propto d^{-1}$, predicts that Δ is affected by the rim over distances far greater than ξ_0, the grain diameter or even the rim width. Since the Golubov model is one-dimensional, and this problem is clearly two dimensional, it is difficult to take this analysis much further. Moreover, the problem discussed here is probably typical of these STJs. It does, however, illustrate nicely how a completely different mechanism than QP loss at the edges, can give rise to the same spatial profile of response inhomogeneity.

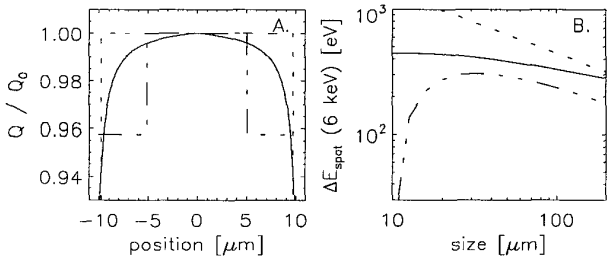

Fig. 8. Illustrations of some phenomenological descriptions of the variation of bandgap Δ as a function of distance d from the edge of the STJ. Two models simply assume a step in Δ, one at 200 nm from the edge (short dash), consistent with Fig. 7a, and one at 4.9 μm (long dash), based on a best fit to the data in Fig. 6a. The other model assumes a more gradual decrease of Δ, based on a powerlaw: $\Delta \propto d^{-1}$ (solid). The left panel shows the resulting variation with position of the charge response in a 20 μm STJ, the right panel the relative variation of energy resolution with device size predicted by these models.

III. Conclusions

The strategy for improving the STJ X-ray energy resolution depends directly on the physical mechanism behind the resolution degradation. QP losses near the edges call for modifications of the fabrication process, while losses into the leads may be remedied by fabricating leads of higher bandgap materials. The analysis of the causes of energy resolution degradation, presented in this paper, has shown that it is not a question of choice between one of the described mechanisms, but that it is important to recognize that several factors are likely to play a role in the resolution degradation of STJs. This explains the persistence of the resolution problem over the past years. In order to solve it, all the key factors must be identified, and their impact on the resolution assessed.

Acknowledgment

It is a pleasure to thank H. Zandbergen of the TU Delft for the TEM images in Fig. 7, M. van den Berg of SRON, Utrecht, for helpful discussions, A. van Dordrecht of ESTEC for invaluable support with the electronics, J. van der Biezen of ESTEC for the microscope images in Fig. 1. The devices discussed in this paper were produced by the Scientific Research Division of Oxford Instruments, Cambridge, UK, and by VTT Electronics, Espoo, Finland.

References

[1] N. Rando et al., *Proc. SPIE 1998*, vol. 3435 (in press)
[2] N. Rando et al., *Proc. SPIE 1998*, vol. 3445 (in press)
[3] P. Verhoeve et al., *these proceedings*
[4] M. Kurakado, *Nucl. Instrum. Meth. Phys.* A 196, 1982, p. 275
[5] N. Rando et al., *Nucl. Instrum. Meth. Phys.* A 313, 1992, p. 173
[6] C.A. Mears, S.E. Labov and A.T. Barfknecht, *Appl. Phys. Lett.* 63, 1993, p. 2961
[7] D.J. Goldie, P.L. Brink, C. Patel, N.E. Booth and G.L. Salmon, *Appl. Phys. Lett.* 64, 1994, p. 3169
[8] R. den Hartog et al., *Proc. SPIE 1997,* vol. 3114, pp. 310-321
[9] P. Verhoeve et al., *Phys. Rev.* B 53, 1996, pp. 809-817
[10] O.J. Luiten et al., *Proc. of LTD-7,* Munich 1997, ISBN 3-00-002266-X, pp. 25-27
[11] M.L. van den Berg et al., *IEEE Trans. Appl. Supercond. 7,* vol. 2, 1996, pp. 3363-3366
[12] J. Martin et al., *Nucl. Instrum. Meth. Phys.* A 370, 1996, pp. 88-90
[13] K. Segall et al. *Proc. of LTD-7,* Munich 1997, ISBN 3-00-002266-X, pp. 47-52
[14] S. Friedrich et al., *Nucl. Instrum. Meth. Phys.* A 370, 1996, pp 44-46
[15] F. Porter, D. Van Vechten, M. Blamire and G. Burnell, *Nucl. Instrum. Meth. Phys.* A 370, 1996, pp. 50-52
[16] N. Rando, P. Verhoeve, A. Poelaert, A. Peacock and D. Goldie, *J. Appl. Phys.* 83, 1998, pp. 5536-5542
[17] D. Lumb et al., *Proc. SPIE 1995*, vol. 2518, pp. 258-267
[18] K. Gray, *Appl. Phys. Lett.* 32 , 1978, pp. 392-395
[19] S. Kaplan et al., *Phys. Rev.* B 14, 1976, pp. 4854-4873
[20] A. Golubov et al., *Phys. Rev.* B 49, 1994, pp. 12953-12968
[21] A. Golubov et al., *Phys. Rev.* B 51, 1995, pp. 1073-1089